Applied Surface Science Advances 23 (2024) 100633

Contents lists available at ScienceDirect

Applied Surface Science Advances

journal homepage: www.sciencedirect.com/journal/applied-surface-science-advances

Full Length Article

# Sand blasting for hydrophobic surface generation in polymers: Experimental and machine learning approaches

Erencan Oranli [a], Chenbin Ma [a,b], Nahsan Gungoren [a], Asghar Heydari Astaraee [a], Sara Bagherifard [a,*], Mario Guagliano [a]

[a] Politecnico di Milano, Via G. La Masa 1, 20156, Milan, Italy
[b] College of Engineering, Nanjing Agricultural University, Nanjing 210031, China

ARTICLE INFO

*Keywords:*
Polymers
Surface treatment
Sand blasting
Wettability
Machine learning

ABSTRACT

Wettability is a crucial surface feature of polymers due to their numerous interaction-destined applications. This study focuses on the application of sand blasting process for investigating the wettability of polymeric materials to produce hydrophobic behavior. Four different polymeric materials, Acrylonitrile Butadiene Styrene (ABS), Poly(methyl methacrylate) (PMMA), Polypropylene (PP), and Polycarbonate (PC) underwent sand blasting with varying process parameters, following a comprehensive plan for the design of experiments. Subsequent analyses included surface roughness measurement and wettability tests, supplemented by scanning electron and confocal microscopy observations to gain deeper insights into the blasted surfaces. A predictive model based on a machine learning algorithm was developed using the backpropagation technique to correlate the surface treatment parameters to surface roughness and wettability indexes. From the experimental results sand blasting proved to be efficient in creating hydrophobic surfaces on all the tested materials. The developed neural network demonstrated high fitting degrees between the predicted and measured values. ABS exhibited the most hydrophobic behavior and emerged as a strong candidate for further investigations.

## 1. Introduction

Surface wettability is one of the key properties for establishing the application of engineering materials. Wettability is defined as the interaction of a solid and a liquid in contact [1,2]. Depending on the application, solid substances can be subjected to measure the wettability with different liquids such as water, oil, etc. In the case of 'water wettability', the corresponding evaluation index is water contact angle (WCA). WCA is a geometrical value depicting the stabilized state of water droplets on a surface, taking a value in the range of 0°–180° [3]. The 90° angle acts as a threshold between the wettability states of hydrophilicity and hydrophobicity.

The main contribution to the wettability of a surface relies upon its chemical composition [4]. The other factor influencing wettability is considered to be the surface physical structure [5]. The wettability phenomenon has been investigated mainly based on two models. Wenzel's model [6] considers the interaction as a sole contact between solid (specimen) and liquid (water). Cassie-Baxter's model [7] further considers the gas state (air entrapped beneath the water droplet) which exists due to the roughness of the free surface. Depending on the surface morphology, the surface state behaves in accordance with one of these models [8].

Surface roughnening is known as a valid strategy for introducing hydrophobicity on a surface [5]. Polymeric materials offer modifiable and reconstructable surfaces and grant a promising option for altering wettability, which has gained significant attention in both scientific and industrial applications [9]. Several surface treatments have been utilized for controlling the wettability of the polymers through surface morphology manipulation including plasma surface treatment [10–17], laser surface texturing [18,19] and sand blasting (SB), that will be more specifically detailed in this paper. Chan et al. [20] mentioned polymers to be suitable candidates for surface treatments because of their initially poor surface characteristics but great chemical and physical properties combined with low cost and availability. They treated polymeric materials with plasma to redefine the surface state in favor of the required level of wettability. Youngblood et al. [21] applied radio frequency plasma treatment on Polypropylene (PP) together with plasma etching of Polytetrafluoroethylene (PTFE – Teflon). The results showed that with

* Corresponding author at: Mechanical Engineering, Polytechnic University of Milan, Via La Masa, Milan, Italy.
*E-mail address:* sara.bagherifard@polimi.it (S. Bagherifard).

https://doi.org/10.1016/j.apsadv.2024.100633

Available online 28 August 2024

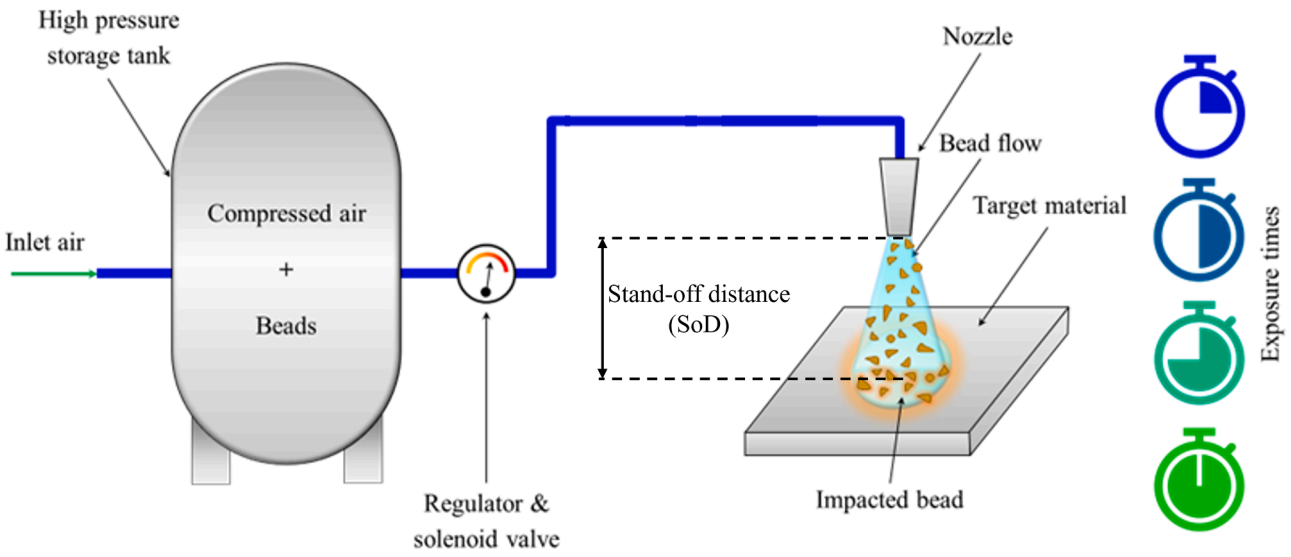


**Fig. 1.** Schematic illustration of the SB process and the main process equipment: regulator & solenoid valve used to control the pressure of the flow through the nozzle.

a roughened surface of PP, a high level of hydrophobicity was retrieved, reaching the level of 170°, which was referred to as ultrahydrophobicity. Another plasma treatment done with argon and oxygen plasma over Polystyrene (PS) and Polyethylene (PE) showed that the increased microwave power led to a decrease in WCA [22]. The effect of final surface roughness on controlling the wettability of the surface was investigated by Sun et al. [23] and it was shown that with the proper control of surface geometry, switching between hydrophilicity and hydrophobicity regimes was addressed on poly(N-isopropylacrylamide) (PNIPA). Nilsson et al. [24] applied sandpaper on Teflon to induce superhydrophobicity with a WCA of 151° In another study by Song et al. [25] on the same material and with the same treatment, abrasive grit size was varied between 120 and 600. The optimum conditions for wettability were obtained with 240-grit size, which was considered as the threshold between Cassie-Baxter and Wenzel states. Menga et al. [26] applied sodium-bicarbonate ($NaHCO_3$) blasting, also referred to as "soft blasting" or "soda blasting", on Teflon as a more autonomous surface treatment. The best state of wettability was obtained with the highest pressure and the lowest stand-off distance (SoD) implemented in the investigation.

Specifically, the technique of SB is identified to be an efficient, cost-effective, and less complex process for altering wettability characteristics. Surface activation of polymers by SB treatment in favor of better functionalization has been the subject of several studies. Chen et al. [27] showed an increase in the tin coating thickness deposited over Acrylonitrile Butadiene Styrene (ABS) and Polyetheretherketone (PEEK) substrates upon surface roughening using SB. Successful surface activation of PEEK was achieved using SB treatment to increase its osseointegration to bone capability [28] as well as improve its biological performance in dentistry [29]. Rocha et al. [30] conducted SB treatment on PEEK using 45-micron-sized alumina media at a pressure of 2.8 bar, a SoD of 10 mm, and an exposure time of 15 s. The outcomes revealed improved adhesion among PEEK, resin cement, and dentin following the treatment, identifying PEEK as a promising material for dental prostheses. Xu et al. [31] analyzed the tensile response of SB treated polyimide (PI) specimens coated with a thin copper (Cu) film and showed that the increased roughness of polyimide by SB led to a decrease in tensile stresses in the Cu films, which in turn reduced the density of surface cracks and increased the ductility of the PI/Cu structure. Zafar et al. [32] investigated the effect of the induced surface roughness using SB on denture fitting surfaces for Poly(methyl methacrylate) (PMMA), with the conclusion that not a very prominent effect was found. Lampin et al. [33] explored the effect of different surface roughness induced on PMMA using SB with varying sizes of aluminum oxide media (50–125–250 μm). The enhanced roughness was found to improve cell adhesion for vascular and corneal explants in correlation with enhanced hydrophobicity.

Although surface functionalization and wettability characteristics of polymeric materials through mechanical surface treatments, particularly SB, have received some attention in the literature, it seems inevitable to conduct systematic research more inclusively, targeting multiple materials highly commercialized in the industry. Furthermore, the chain-like relation among the intrinsic properties of the material, processing parameters of surface treatment, final surface morphology, and wettability leads to an undeniable demand for developing an appropriate predictive model using machine learning (ML) techniques such as artificial neural networks (ANN). Developing predictive models is a strategic approach to optimize costs by significantly reducing the number of experiments and material consumption [34–37].

In this study, SB surface treatment was conducted on several polymers with varying process parameters to induce different levels of surface roughening. Such a variety of final surface roughness was targeted for providing insights regarding the effect of roughness on the wettability of the material as an objective of the current study. SB using alumina media was selected due to its better recyclability and less risk of contamination in the case of polymers compared to soft blasting. The performance of the treated surfaces was explored using consecutive surface roughness measurements and wettability tests. The outcomes were utilized to discuss the suitability of SB treatment for realizing hydrophobic surfaces on polymers. Furthermore, the study was also motivated by observing the wetting behavior of different polymers such that promising candidates can be opted for future research on the topic. Experimental results were used as datasets to analyze the wettability of the treated surfaces by developing an ANN model, which was constructed based on the SB process parameters as inputs and surface roughness (Ra, Rq) and final WCA as outputs. The model parameters were optimized using the backpropagation technique. The predictability of the developed model was discussed using separate experimental tests.

## 2. Materials and methods

### 2.1. Materials and sand blasting

Thermoplastic polymers, namely ABS, PMMA, PP, and

**Table 1**
SB process parameter levels for the design of experiments (DOE).

| Airflow pressure (bar) | Exposure time (s) | Stand-off distance (mm) |
|---|---|---|
| 4 | 3 | 90 |
| 5 | 6 | 120 |
| 6 | 9 | 150 |
| – | – | 180 |

Polycarbonate (PC), were selected as the substrate material in this study for their high plastic deformability at room temperature with minimum risk of damaging the surface, together with relatively high ultimate tensile strength and low cost. The samples of all the materials were cut into squares of 40 mm x 40 mm. SB was done with a Guyson Formula F1600 cabinet-type blasting machine. Aluminum oxide (Al2O3) with an average particle size of 1 mm was used as the blasting media. High hardness and better mechanical properties of the media compared to substrate materials ensured a reliable treatment with high recyclability. A schematic of the SB process together with the main process equipment is depicted in Fig. 1. A pressure-adjustment valve was used to control the pressure of compressed air provided through a central system with a 7-bar input value. Further details on the process can be found in a previous study [38]. The main processing parameters were considered to be the pressure, exposure time (t), and SoD. Three levels of air pressure, three levels of exposure time, and four levels of SoD were considered to differentiate the effect of each variable, considering a full factorial design of experiments (DoE) plan. Table 1 summarizes the selected levels for each process parameter. The blasted surfaces were cleaned with ethanol in an ultrasound-cleaning system for two min to remove possible contamination from SB on the treated surface.

### 2.2. Roughness measurement

Blasted samples were cut into 20 mm x 20 mm squares for the subsequent measurements. Mahr PGK Perthometer – Surface Probe MFW-250 was used for measuring the surface roughness profile. A cut-off wavelength of 0.25 mm was used to exclude the waviness from the primary profile and 2 μm was selected as the diameter of the measuring probe. To address the variability of the roughness, it was evaluated at 3 independent regions of the sample far from each other. Measurements were done in accordance with the standard ISO-4288 [39].

### 2.3. Wettability tests

WCA measurements were conducted with a Rame-Hart model I00–00 230 contact-angle goniometer. Distilled water was used as the droplet and the volume of each droplet was kept at ~8 μl. An average WCA was calculated over 8 measurements using four droplets (on both sides) to characterize the overall state of wettability. One separate droplet was put at the center of the specimen to visually confirm the level of wettability between the edges and the center. A representative image for WCA measurements can be seen in Fig. 2.

### 2.4. Characterization of surface morphology of the blasted surfaces

A Zeiss EVO-50 scanning electron microscopy (SEM) was utilized to examine the top-surface morphology of the specimens. The high irregularity of the impacting media in addition to the quick and intense deformation of polymers under even low exposure times increased the randomness of the surface roughening. Surface digitalization was done using Alicona InfiniteFocus G4 in order to make a comparative analysis of different materials treated by SB treatment.

### 2.5. Predictive model with ML algorithm

Based on the experimental results for each material, a Matlab subroutine was developed to train a feedforward neural network (FNN). Within this function, both feedforward and backpropagation methods were employed. The traincgf network training function was used, which is based on a conjugate gradient method with Powell-Beale Restarts. This particular algorithm incorporates the Powell-Beale restart strategy

**Table 2**
Line profile roughness parameters according to ISO 4288 standard.

| Parameter notation | Description | Formula |
|---|---|---|
| Ra | Arithmetical mean of absolute values of entire roughness data over evaluation length | $=\frac{1}{L}\sum_{i=1}^{L}\lvert Z_i\rvert$ |
| Rq | Root mean square of entire roughness data over evaluation length | $=\sqrt{\frac{1}{L}\sum_{i=1}^{L}Z_i^2}$ |

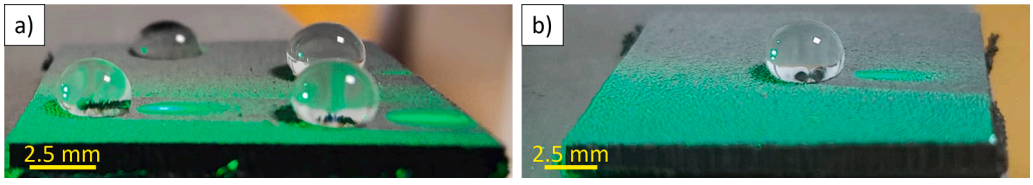


**Fig. 2.** Wettability test configuration: a) four droplets on different positions of the specimen surface b) a visual confirmation with a droplet in the center.

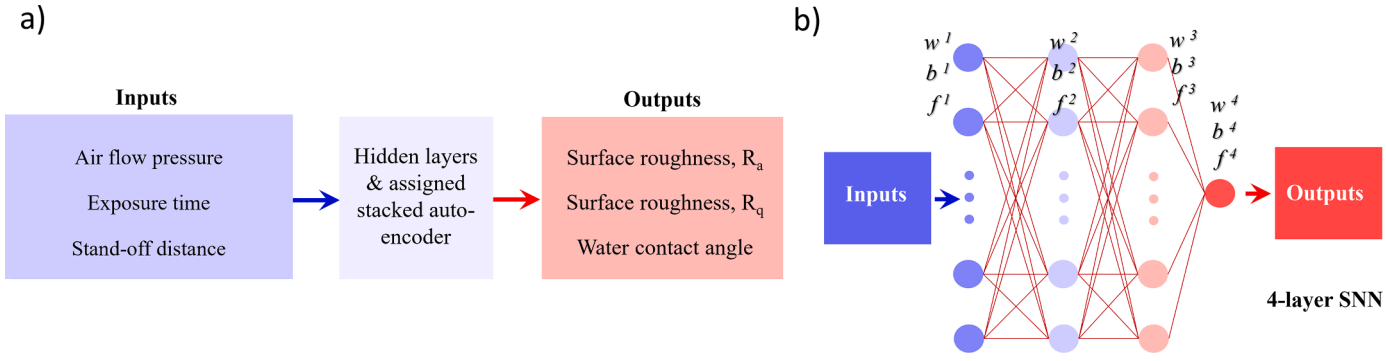


**Fig. 3.** Inputs and outputs of ML algorithm.

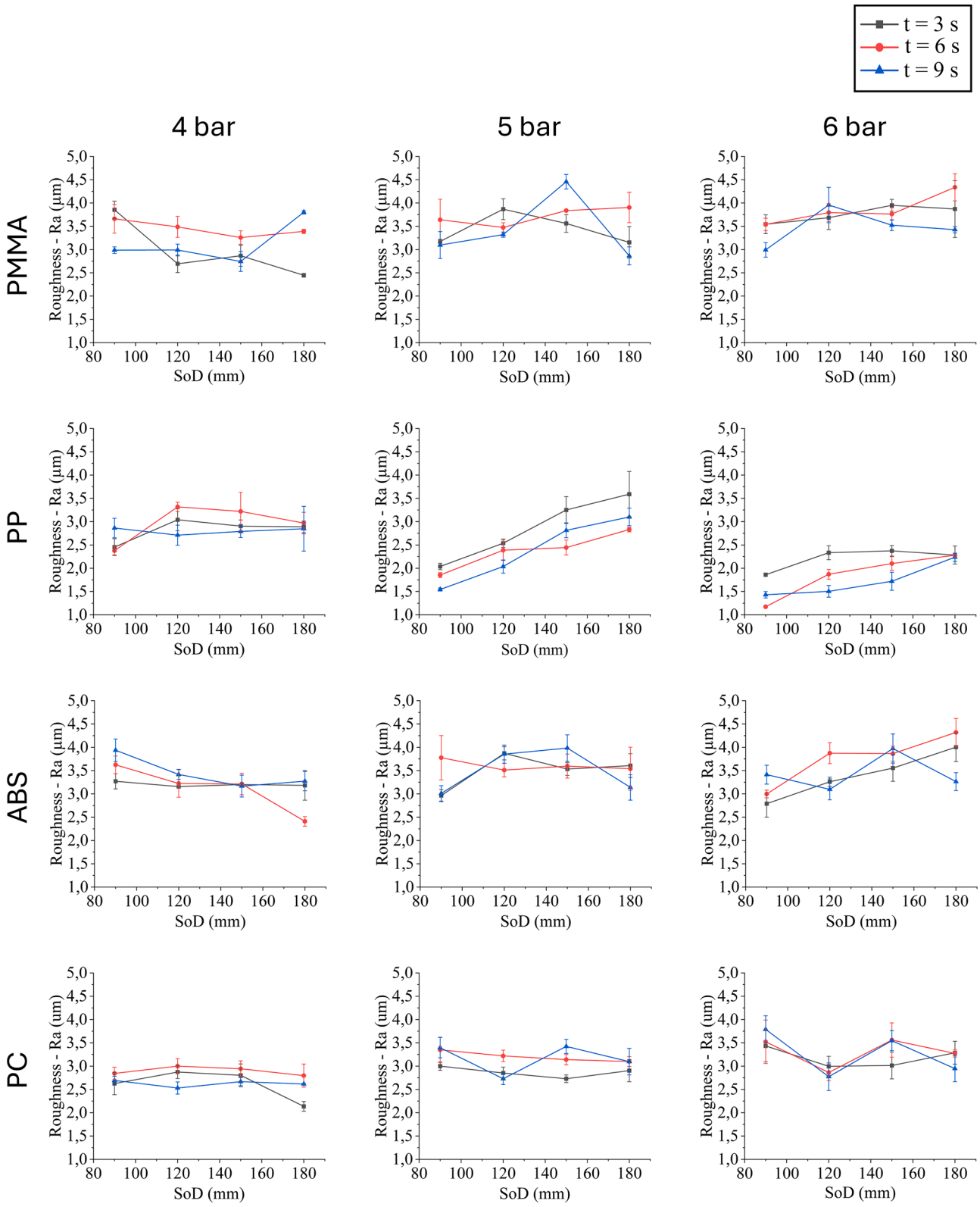


**Fig. 4.** Surface roughness (Ra) as a function of stand-off distance after sand blasting at air pressure levels of 4, 5, and 6 bar for PMMA, PP, ABS, and PC.

to enhance the efficiency of the gradient descent algorithm.

The model's inputs included SoD, airflow pressure, and exposure time, while the outputs consisted of surface roughness metrics (Ra, Rq) and surface WCA. During the training steps, to get the best performance of the FNN, a grid search was employed, and the training process was conducted for varying numbers of hidden layers and different numbers of neurons of each layer. Considering the computational efficiency, the number of neurons per layer commenced at 6 during the grid search. Each time after network training and evaluation, the $R^2$ value showing the quality of fitting was recorded. Fig. 3 shows the methodology followed for the construction of the ML algorithm. The steps followed for building the ML algorithm are summarized below:

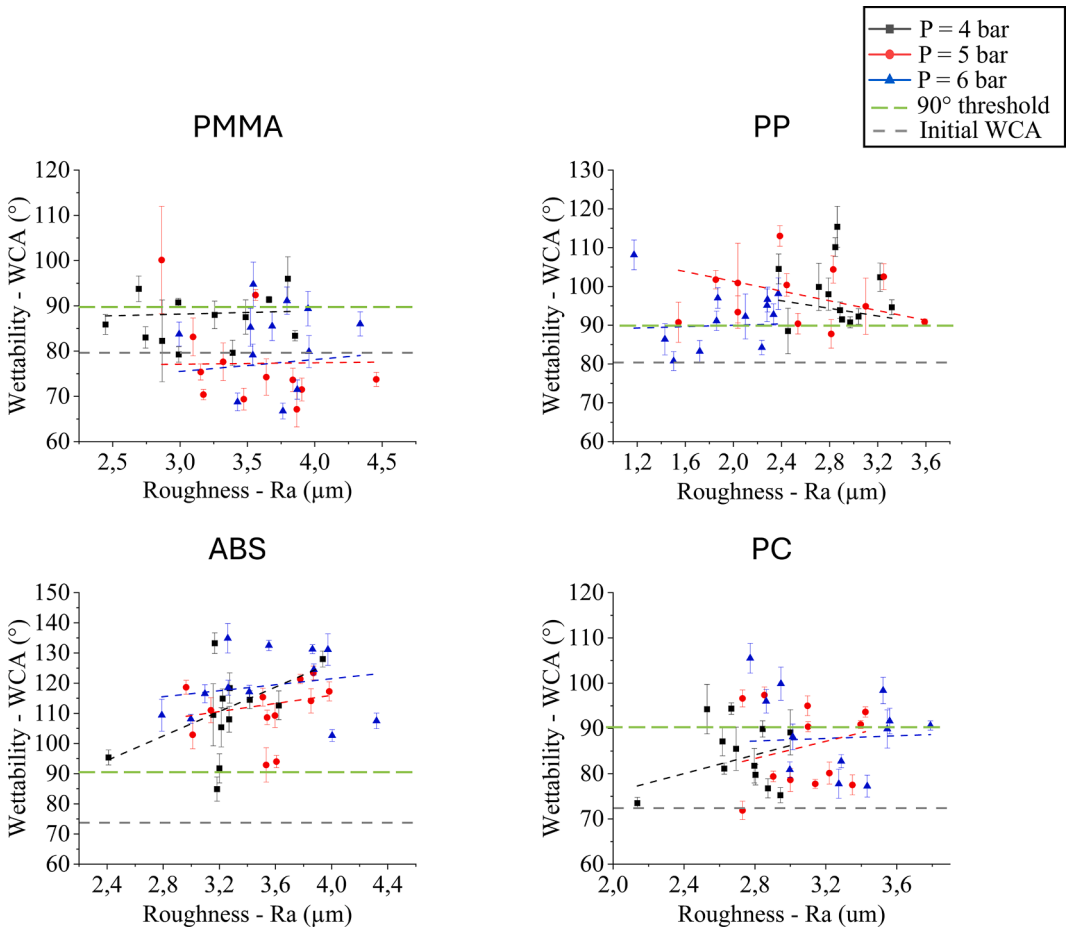


**Fig. 5.** Wettability (WCA) vs. surface roughness (Ra) for PMMA, PP, ABS, and PC.

1. Extraction of the experimental data, taking the cosine of the contact angle value and then normalization.

2. Separation of the data sets. In this study, out of 36 samples for each material, 25 were used as the training set (70 %), 6 as the validation set (15 %), and 5 as the test set (15 %).

3. Selection of appropriate network parameters (training function, learning rate, the index of training data, validation data, and test data).

4. Analysis of the performance of the network with different numbers of hidden layers (1, 2, 3, 4, 5) and selection of the optimal network framework by comparing the correlation coefficient $R^2$. The number of neurons per layer was retrieved starting from 6 and increasing by 6 each time until it reached 54.

5. The $R^2$ values were obtained for each training and the maximum $R^2$ value was recorded. The corresponding network with the highest $R^2$ was recorded for further exploitation.

6. Analysis was conducted based on the model.

## 3. Results and discussion

### 3.1. Surface roughness results

The surface roughness parameters considered for evaluation here are decided to be the global parameters, i.e., the average of absolute values of the roughness profile Ra and the root mean square of the roughness profile Rq, as formulated in Table 2. The roughness profile is represented with $Z$ and the total length of the measurement is $L$. Other roughness parameters characterized by local features such as maximum peak-to-valley distance, the height of the longest peak, and the height of the deepest valley are not considered, especially considering the highly irregular geometry of the blasting media.

Fig. 4 depicts the surface roughness Ra parameter as a function of SoD at three levels of air pressure (4, 5, and 6 bar) and exposure times (3, 6, and 9 s) for PMMA, PP, ABS, and PC polymers. For the sake of brevity, only Ra values are plotted since similar trends were observed between the two examined statistical outcomes (Ra, Rq) of the final surface roughness states. One sample was blasted per each combination of process parameters with the corresponding pressure, exposure time and SoD variables. For each sample, 3 roughness measurements were conducted on different linear profiles. Standard error was calculated and demonstrated out of three measurements using the error bars in Fig. 4. The average Ra values fall roughly in the relatively wide range of 1 to 4.5 µm for the investigated material-processing parameter combinations starting from a roughness close to zero (Ra values in the range of 0.05–0.15 ± 0.02 µm) on the untreated materials. The wide range of roughness values obtained after SB was induced by the multiple combinations of process parameters as they were able to generate such a diverse range of surface roughness. Due to the intrinsic features of the sand blasting process, fluctuations of roughness are inevitable. The reported error values are mostly lower than 0.5 µm. Lampin et al. [33] also reported Ra values of 3.34 ± 0.54 µm on PMMA after sand blasting with 0.25 mm Alumina particles and a pressure of 4 bar.

Furthermore, the induced surface roughness is an interplay between the processing parameters of the SB process on one hand and the material properties of each polymer, especially its dynamic deformation characteristics under SB, on the other hand. In general, no unique trend is observed between the Ra parameter as a property defining the topography and the main SB process parameters. This is explainable regarding the competing factors that influence the surface morphology and roughness. As with any other surface peening method, the media characteristics, its flow intensity and surface coverage of the SB process

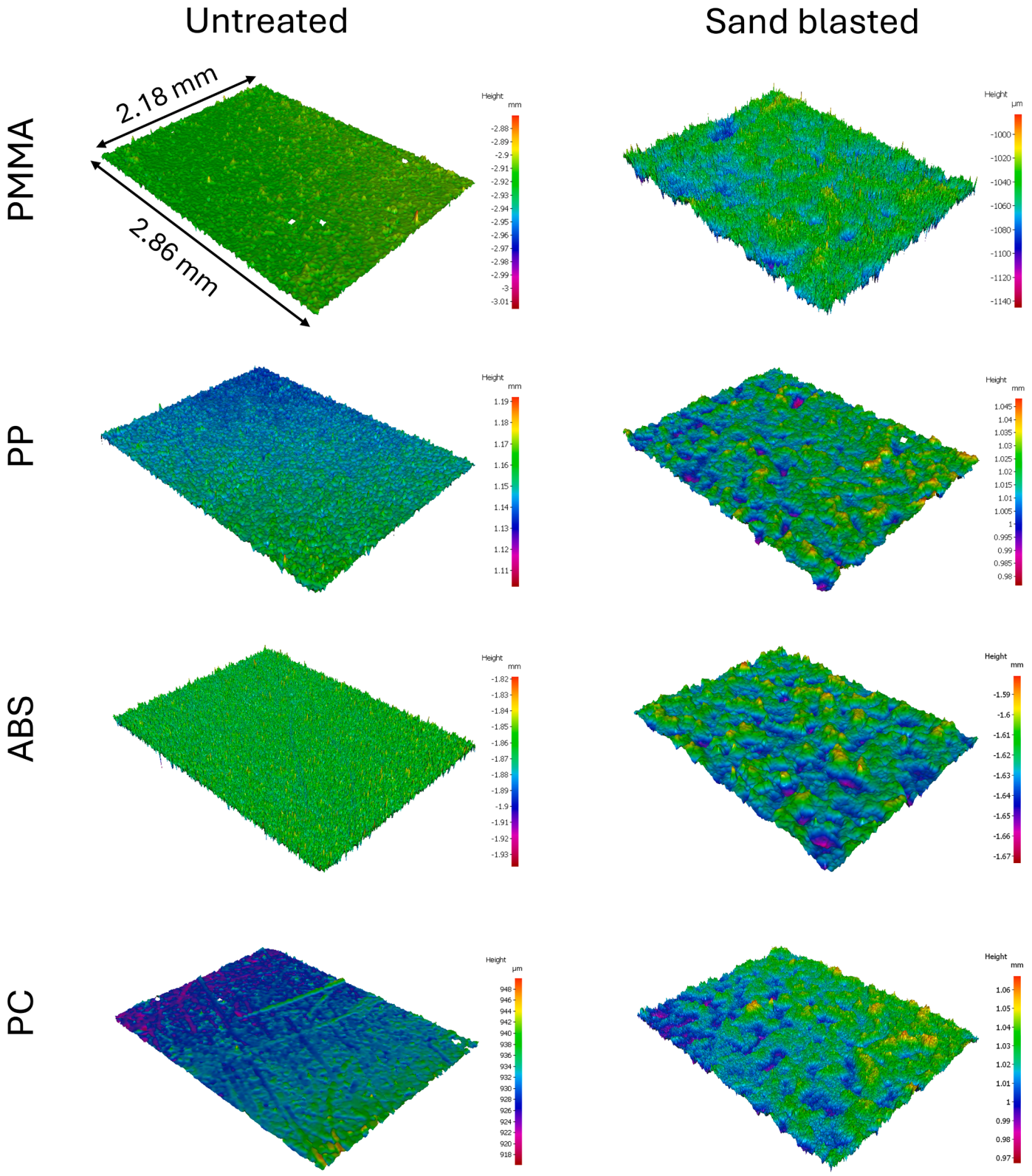


**Fig. 6.** 3D images of the untreated and sand blasted surfaces having the highest roughness for PMMA, PP, ABS, and PC.

define the contribution of the processing parameters to the induced roughness. Considering that the same media was used in all cases, as a general behavior, a higher flow intensity and coverage can lead to higher surface roughness [40]. However, sometimes, the roughenss may saturate with a further increase in the intensity or coverage [41]. The flow intensity (also known as Almen intensity) is governed by the media velocity and size. The media velocity is dependent on the SoD, usually increasing immediately after the nozzle exit, reaching a maximum, and then falling slightly at larger SoDs [42–44]. The surface coverage, on the other hand, depends on many factors such as substrate material properties, the exposure time, and the media mass flux which, in turn, is a function of the SoD. As an instance, an increasing SoD may vary the

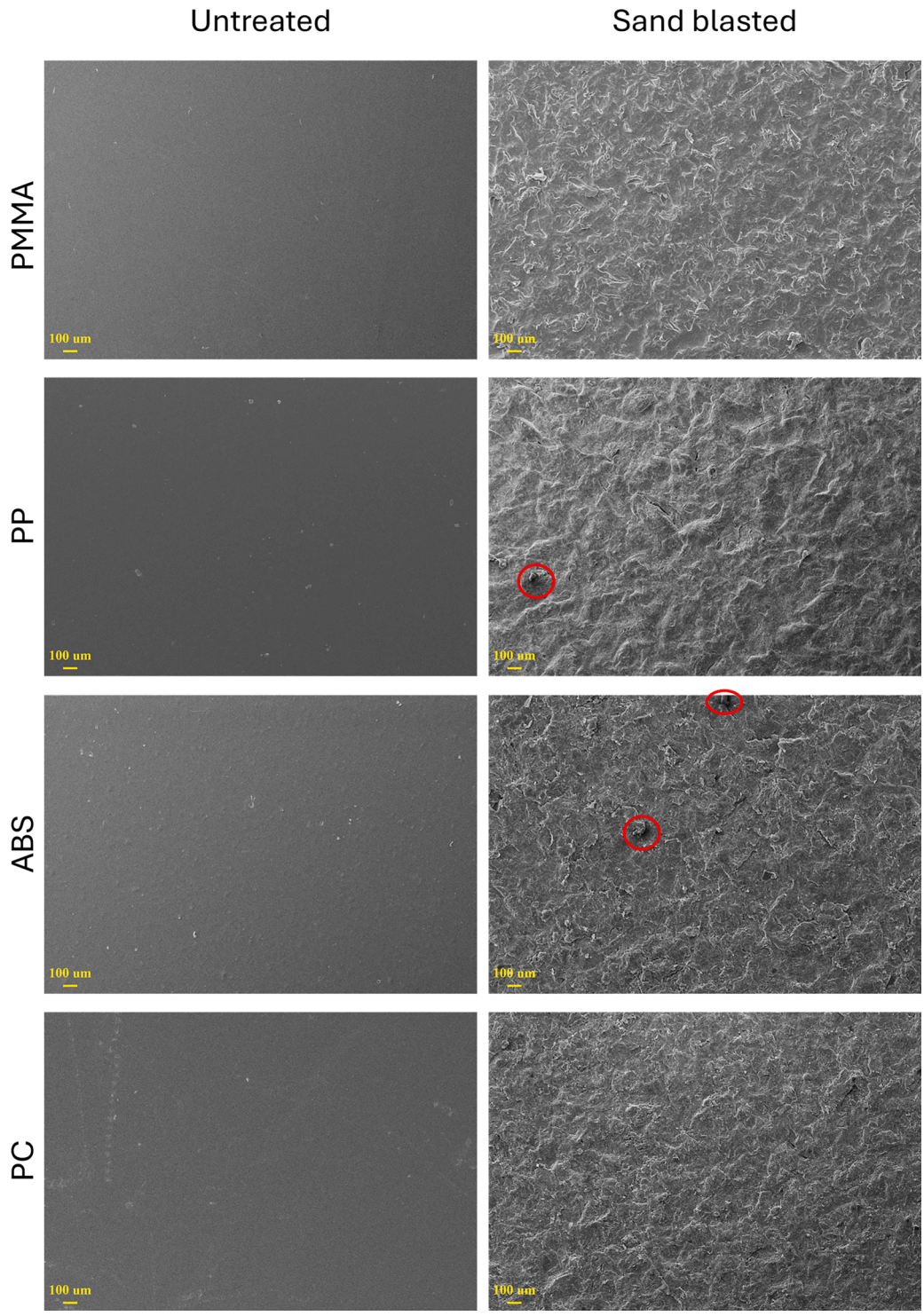


**Fig. 7.** SEM images of untreated and sand blasted surfaces having the highest roughness for PMMA, PP, ABS, and PC.

intensity and coverage in the opposite direction, increasing the first one and reducing the second one such that the overall influence on the roughness may not be easily anticipated.

Another observation in Fig. 4 is on the effect of the material on the complexity of prediction. By examining the plots, it is found that in some cases there can be realized a maximum Ra at a certain air pressure within the applied SoD span. For instance, in the case of PMMA blasted at an exposure time of 9 s, this maximum moves to lower SoDs with increasing air pressure. Instead, for PP and ABS, the maximum Ra at the same exposure time occurs at larger SoDs with increasing pressure while for PC, there seems to be no relevant maximum Ra since either the roughness does not change so much or fluctuates a lot with increasing SoD. The relatively high variation in the induced surface roughness and the complex interplay of the SB process parameters is evident from the plots in Fig. 4 and motivates further the development of a predictive model, able to consider the intricate interaction of the most affecting parameters on the output roughness.

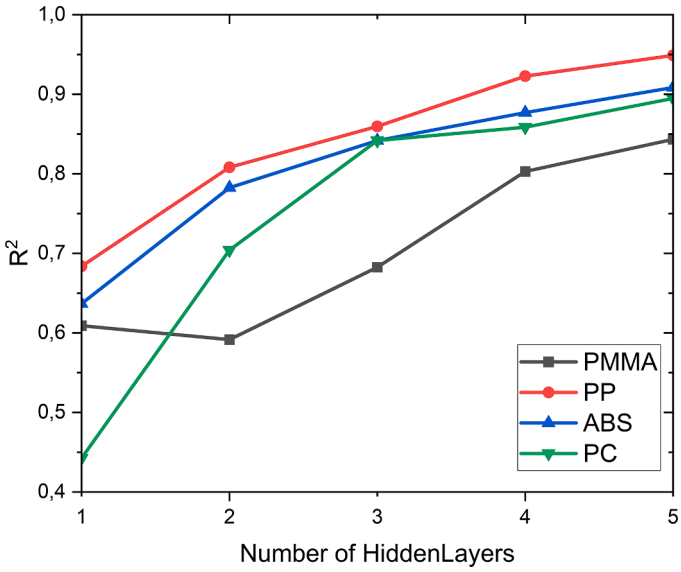


**Fig. 8.** Correlation coefficient $R^2$ values of the networks with different numbers of hidden layers for different materials.

### 3.2. Wettability results

The wettability results in terms of WCA are reported in Fig. 5 as a function of the surface roughness parameter Ra. It is noted that a separate marker type is presented for each air pressure level since it will be designated as the major process parameter affecting the wettability in the later sections of this study. WCA measured on PMMA are observed to mostly fall close to the initial WCA (~ 80°), fluctuating between higher and lower hydrophilicity conditions with less predictable trends. It is also noted that only a few of the processing conditions provided hydrophobicity, passing the threshold of 90°. For the PP material as evidenced by WCA results (Fig. 5), the initial WCA (~80°) exceeded in almost all the blasting conditions and the hydrophobicity was also achieved by a maximum average WCA of ~115°.The ABS has the highest WCA results on average, as observed in Fig. 5. While all the final WCA values exceeded the initial wettability angle (~73°), the general tendency is also observed to be hydrophobic in the final state. Among the examined materials, ABS is one of the materials with relatively low mechanical properties (yield strength of 30 MPa [45]) and low initial WCA (73°). Relatively lower yield strength allows more severe deformation under the same SB process conditions, which might have contributed eventually to the lower wettability. As regards PC material, almost all blasting conditions resulted in a WCA higher than the initial WCA (72°). In this case, the SB process was able to induce hydrophobicity with the maximum average WCA of 105°.

The comparative trends of wettability and roughness against the air pressure are investigated according to the least squares fitting lines in the plots (Fig. 5). Although the data scatter is large, it still can help assessing the trends for different materials comparatively. The fitting lines for different pressure levels indicated approximately similar trends (decreasing or increasing) for each corresponding material. The examination of the trends suggests that the roughness has a negligible effect on the wetting behavior of PMMA. The trend lines of PP have mostly decreasing wettability with increasing roughness even if most of the results are observed to be above the 90° threshold. This suggests that in the range of the applied pressure, the WCA of PP already provided a maximum value, and a further increase in the pressure is not expected to bring any benefit in favor of higher hydrophobicity. ABS seems to be the most rewarding material not only in terms of remarkable WCA results, but also on the overall trend of such behavior as all the trend lines have the highest slopes when compared to the rest of the materials. Furthermore, the WCA results would be expected to increase, possibly beyond the level of superhydrophobicity (>150°) with more deformation induced on the surface. PC showcased a roughly increasing trend, which led the results to remain in the window between the initial state and the threshold for wetting behavior change.

### 3.3. Surface morphology of blasted surfaces

The 3D images taken with Alicona InfiniteFocus G4 microscope are reported in Fig. 6 for the untreated and treated surfaces. For a more clear presentation of the surface morphology, images are presented with 3X magnification. A much rougher and more irregular surface morphology is induced upon the application of SB with respect to the initially flat surfaces for all the studied materials, as discussed in Section 3.1. By examining and comparing the initial and the treated morphologies, it is found that the initial morphology in the untreated condition is very homogeneous over the entire sample's surface. The roughened surfaces indicate a less homogenous morphology which is dependent on the level of stability of the process, and irregular treating media, peculiar to peening-based treatments [40]. This can explain, to some extent, the relatively large variability observed in the surface roughness and the resultant wettability as indicated in Fig. 4 and Fig. 5.

SEM observations performed on the untreated as well as sand blasted surfaces having the highest surface roughness are reported in Fig. 7. While the untreated surfaces show a high degree of homogeneity and regularity, the blasted conditions are characterized by irregular and less homogeneous surfaces for all the examined materials.

Highly irregular final surface morphology is observed for all cases, falling in the expected trend after SB treatment with geometrically heterogeneous impacting media. A degree of surface contamination by the blasting media can also be assumed even after cleaning. It is known that the risk of contamination has a negative correlation with the particle size and with increased media size, this risk can be reduced. [46] In this regard, SB treatment with an average particle size of 1 mm was not expected to bring a high risk of contamination. Alumina contamination from SB media is highlighted in Fig. 7 which was found to be negligible in amount and thus, no appreciable effect can be imagined on the wetting performance. Even if this contamination could affect the final wettability characteristics, it is considered a dependent variable to the processing parameters, and thus, will not be examined deeply here.

### 3.4. ML results

Fig. 8 depicts the correlation coefficient $R^2$ values of the ANN model trained with different numbers of hidden layers (nHs). Since there are three different outputs, each characterized by its individual $R^2$ value, the minimum $R^2$ value among the three was adopted as the benchmark for assessing the network's performance capability. As observed, the $R^2$ values exhibit an increasing trend with the growing nHs. For a single hidden layer, the $R^2$ values for ABS, PC, PMMA, and PP were 0.64, 0.44, 0.61, and 0.68, respectively. Subsequently, with an increase in nHs, the $R^2$ values experienced a sharp initial rise, followed by a gradual increase, eventually reaching 0.91, 0.89, 0.84, and 0.95, respectively. Upon comparing the $R^2$ values under nHs of 4 and 5, minimal differences were observed. Considering the computational efficiency, here we opted for nHs to be 4.

Under the condition of nHs being 4, four ANNs with hidden layer structures of [36 42 42 6], [30 42 36 30], [54 12 30 18], and [24 48 24 12] were established. Fig. 9 illustrates the regression coefficients of these FNN models, while Fig. 10 presents a comparative analysis between the model predictions and experimental data for WCA, Ra, and Rq. As shown in Fig. 9, almost all data points are distributed near the dashed line, which represents the equality of experimental and predicted results. In addition, the test sets exhibit high $R^2$ values, with $R^2$ values for ABS and PP surfaces reaching 0.99938 and 0.99569, respectively. These results indicate that the developed models have excellent predictive accuracy for WCA, Ra, and Rq on the treated surfaces of the

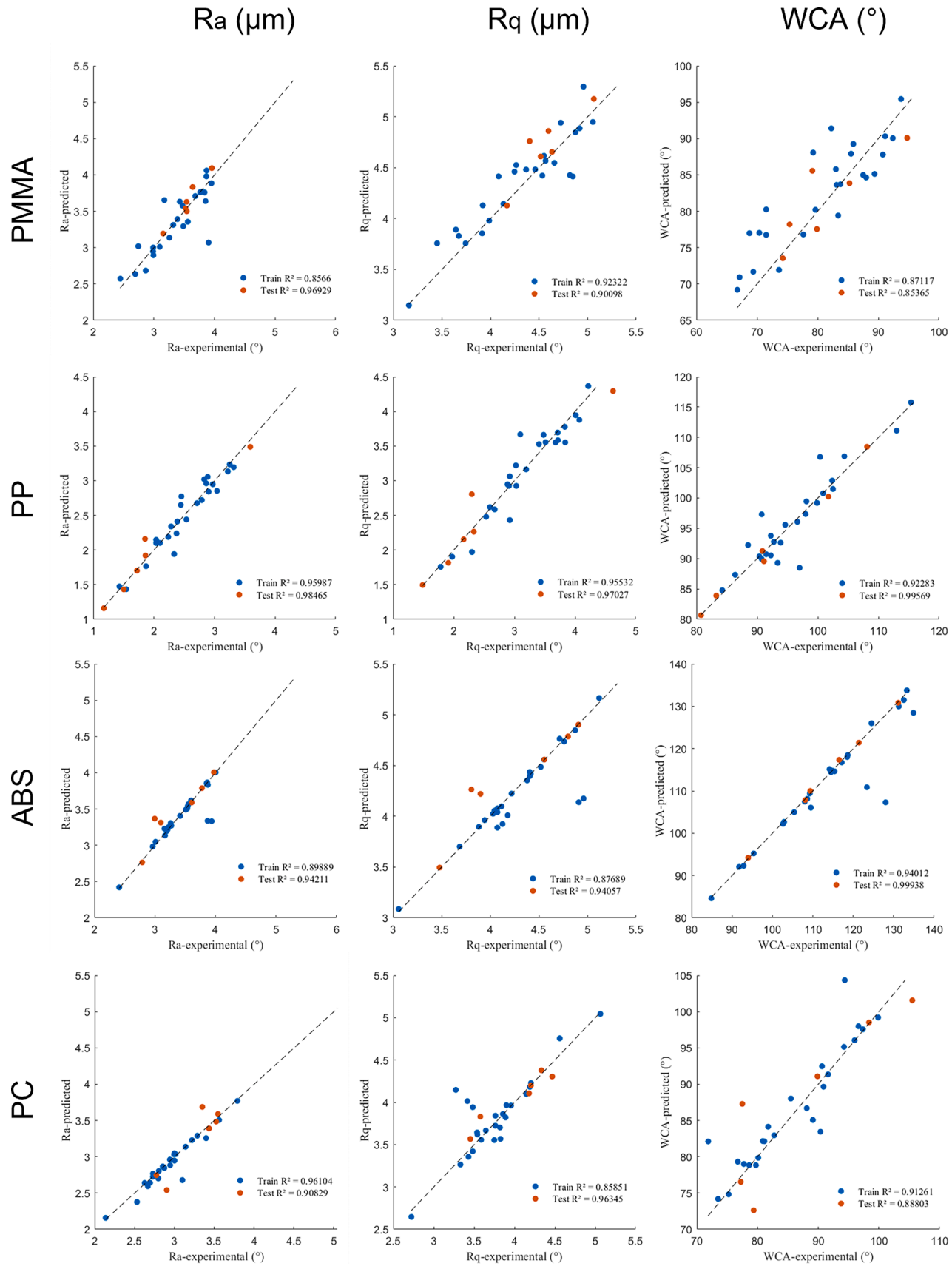


**Fig. 9.** Regression coefficient ($R^2$) of the model: $R^2$ values calculated via the train data set are marked as train $R^2$, and those calculated via the test data set are marked as test $R^2$. The dashed line represents the equality of experimental and predicted results.

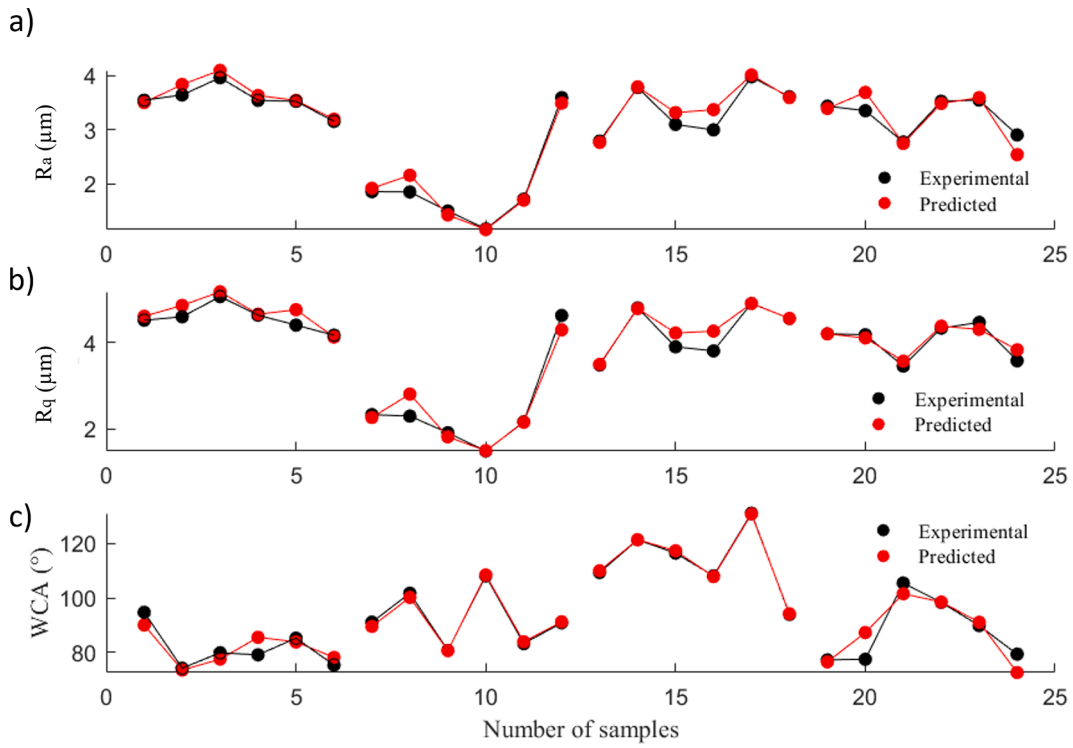


**Fig. 10.** Comparison of FNN predictions with experimental data for Ra (a), Rq (b), and WCA (c); 1–6 for PMMA test group, 7–12 for PP test group, 13–18 for ABS test group, and 19–24 for PC test group.

studied materials. The scatter plots in Fig. 10 compare the experimental data with the prediction results of the FNN models, demonstrating the efficacy of the proposed model in predicting the results closely aligned with experimental values. Furthermore, the results observed in Fig. 10 indicate that experimentally derived Ra and Rq exhibit similar trends, with the predictions closely corresponding to the experimental results.

Fig. 11 shows the 2D contour plots generated based on the FNN model obtained from training for PMMA, PP, ABS, and PC, respectively. Examination of the obtained plots leads to a way for evaluating the air flow pressure as the largest influencing factor. The plots are arranged in a systematic order to investigate the coupled effects of air pressure – SoD (top), air pressure – exposure time (medium), and exposure time – SoD (bottom). The evaluation indexes of Ra, Rq, and WCA are given, respectively, from left to right.

As regards PMMA, the roughness parameters Ra and Rq increase with an increase in pressure, but the WCA decreases up to the level of 5.2 bar and then increases with an increase in pressure. Furthermore, Rq initially increases and then decreases with exposure time. However, its WCA is not significantly correlated with either exposure time or SoD. Conversely, for the blasted PP surfaces, both roughness parameters (Ra and Rq) decrease with increasing pressure. Since the WCA shows a close trend, it can be deduced that surface roughness and wettability had similar responses to the treatment. The effect of the remaining parameters can also be realized such that WCA increased with exposure time and decreased with SoD. In the case of ABS and PC materials, the Ra, Rq, and WCA gradually increased with an increase in pressure. For ABS, a larger SoD and longer exposure time correlate with higher WCA, Ra, and Rq. For PC, both WCA and Ra increased with exposure time. However, as the SoD increased, Ra showed a decreasing tendency. In summary, it is deduced that during SB treatment, pressure has a greater effect on WCA, Ra, and Rq, while the complex effects of SoD and exposure time on the surface characteristics of various polymers investigated here can be attributed to the differences in the original material properties.

In this study, the number of data points to be used for the ML algorithm is constrained by the experimental conditions and available resources; however, while recognizing the limitations of the developed ML algorithm, we have tried to ensure its predictive efficacy by conducting a comprehensive assessment, evaluating the $R^2$ of the training set and the testing set, comparing the testing set results with the actual results, and performing heat value analysis to assess grid performance. Thus we believe that this research can yield valuable insights into analyzing the effects of sand blasting processes on the roughness and wettability of various polymer materials.

## 4. Conclusions

In the light of the industrial tendency to the surface functionalization of polymeric materials, an experimental campaign was created and followed where PMMA, PP, ABS, and PC polymers were subjected to sand blasting. The study has been conducted systematically, comprising the selection of suitable materials and varying the effective process parameters concerning a full-DoE plan. The evaluation indexes were regarded as the final surface roughness and wettability evaluated through water contact angle (WCA) tests. A machine learning algorithm was built and optimized to act as a predictive interface. The concluding remarks are listed below:

- Sand blasting process proved to be an efficient method for generating hydrophobic surfaces on the selected polymeric materials. Only in the case of PMMA, some process parameter combinations contributed to more hydrophilicity than the initial state.
- ABS was identified as the strongest candidate for generating hydrophobic surfaces (WCA of 133°) among the investigated materials. This particular response was attributed partly to the relatively lower yield strength of the material, which granted more severe deformations at room temperature.
- The FNN model was applied to the performance analysis of sand blasting and the model with a high correlation coefficient ($R^2$) was obtained by optimizing the framework. The model correlation coefficients obtained from shallow neural networks (comprising one or

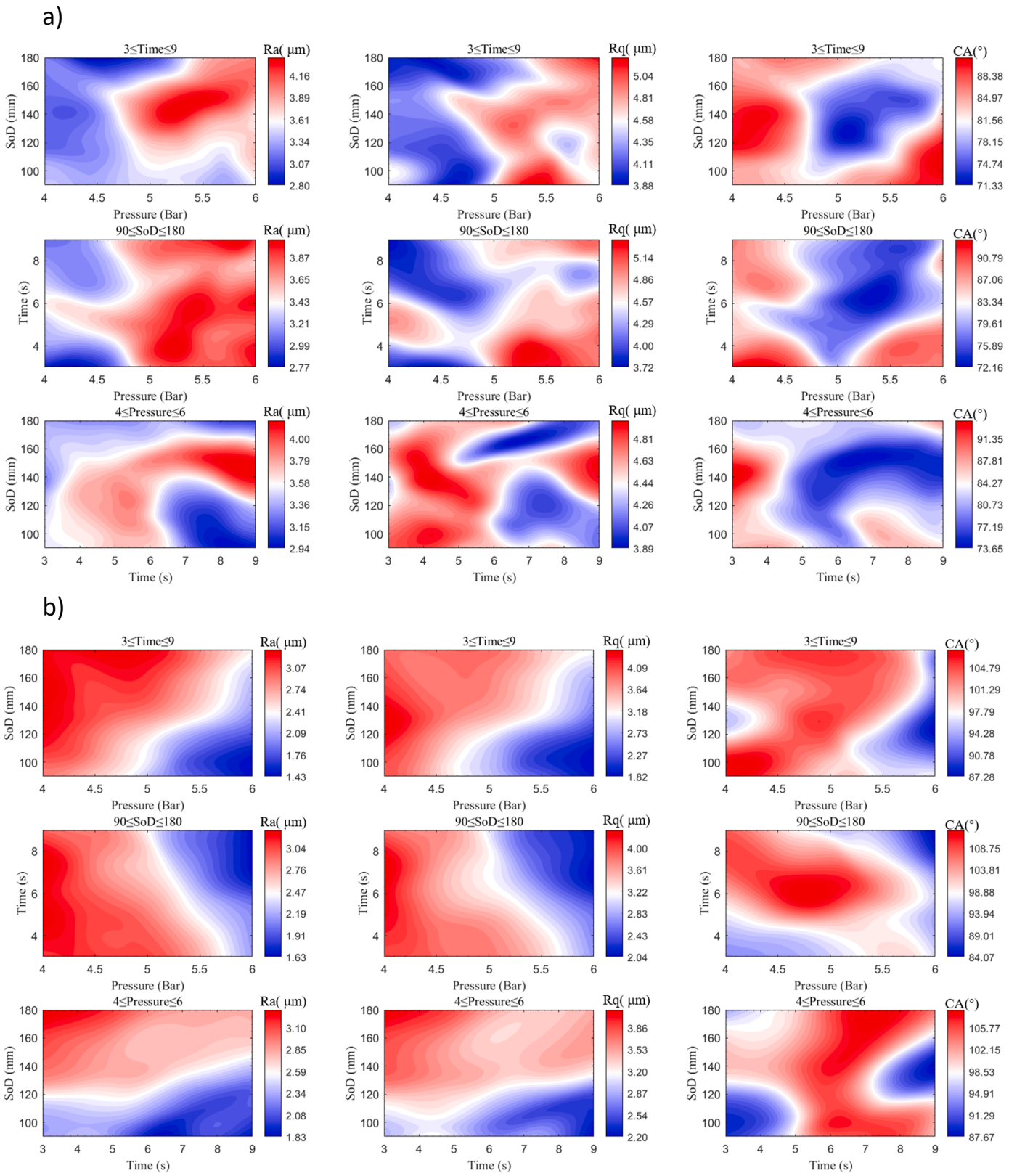


**Fig. 11.** 2D contour plots regarding the influences of the effective parameters of the SB process for a) PMMA, b) PP, c) ABS, d) PC.

two hidden layers) were low, whereas increasing the number of hidden layers optimized the prediction results of the model, and the $R^2$ value was increased to levels higher than 90 %. Evaluation of the model with regard to further expanded experimental tests helped optimize the model effectively.

- Based on a developed feedforward neural network (FNN), the relationship between the blasting process parameters, surface roughness,

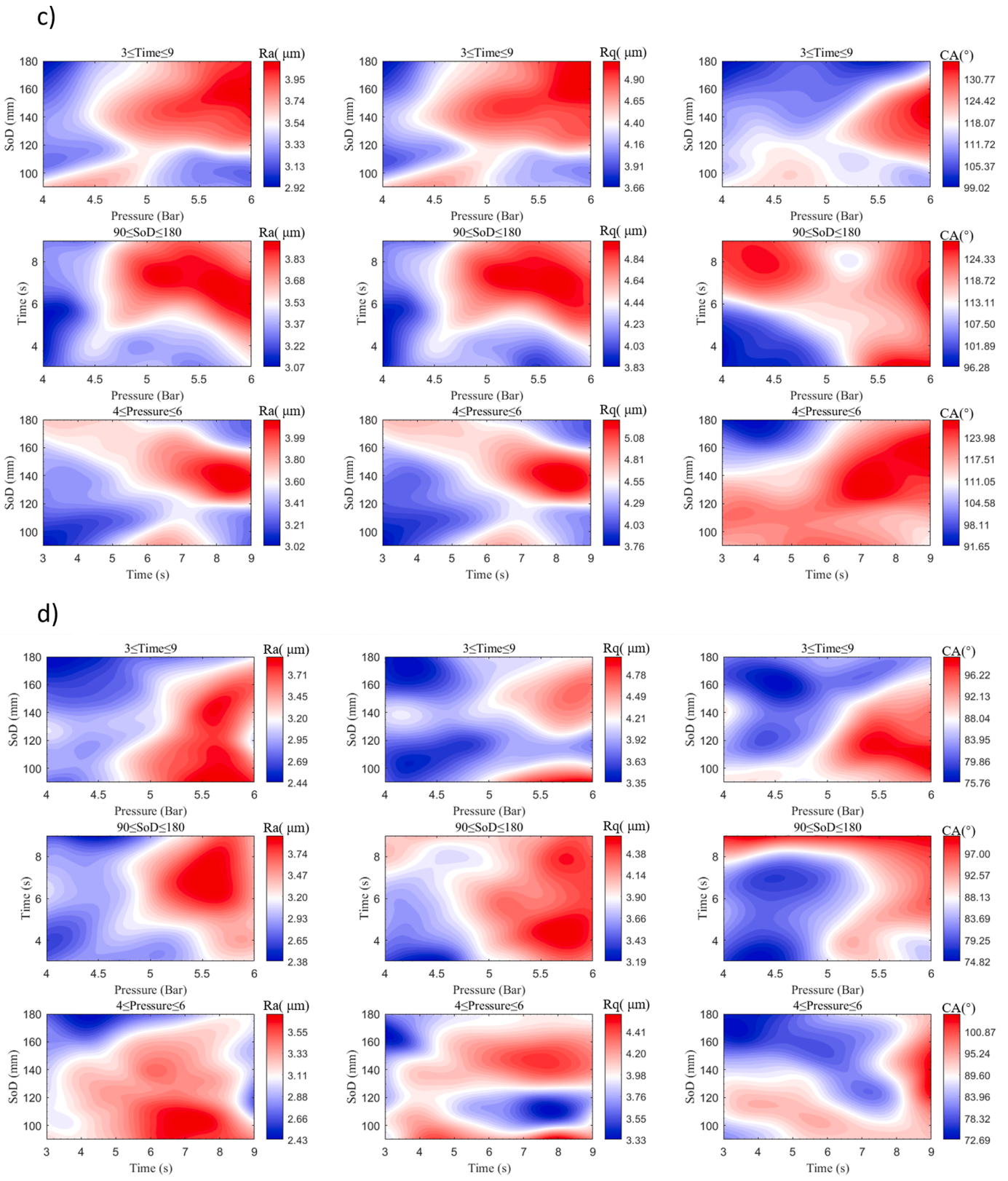


**Fig. 11.** (*continued*).

and WCA was successfully examined. The factor having the highest influence on WCA and surface roughness was identified to be air flow pressure.

## CRediT authorship contribution statement

**Erencan Oranli:** Writing – original draft, Visualization, Investigation, Formal analysis. **Chenbin Ma:** Writing – original draft, Visualization, Investigation, Data curation. **Nahsan Gungoren:** Investigation,

Data curation. **Asghar Heydari Astaraee:** Writing – review & editing, Methodology, Formal analysis. **Sara Bagherifard:** Writing – review & editing, Supervision, Conceptualization. **Mario Guagliano:** Writing – review & editing, Supervision, Methodology.

## Declaration of competing interest

The authors declare that they have no known competing financial interests or personal relationships that could have appeared to influence the work reported in this paper.

## Data availability

Data will be made available on request.

## Acknowledgment

C.M. would like to thank the China Scholarship Council for the financial support (CSC, No.202206850066).

## References

[1] T. Darmanin, F. Guittard, Wettability of conducting polymers: from superhydrophilicity to superoleophobicity, Prog. Polym. Sci. 39 (2014) 656–682, https://doi.org/10.1016/j.progpolymsci.2013.10.003.
[2] C.G. Jothi Prakash, R. Prasanth, Approaches to design a surface with tunable wettability: a review on surface properties, J. Mater. Sci. 56 (2021) 108–135, https://doi.org/10.1007/s10853-020-05116-1.
[3] A. Marmur, C.Della Volpe, S. Siboni, A. Amirfazli, J.W. Drelich, Contact angles and wettability: towards common and accurate terminology, Surf. Innov. 5 (2017) 3–8, https://doi.org/10.1680/jsuin.17.00002.
[4] P.G. de Gennes, Wetting: statics and dynamics, Rev. Mod. Phys. 57 (1985) 827–863, https://doi.org/10.1103/RevModPhys.57.827.
[5] L. Feng, S. Li, Y. Li, H. Li, L. Zhang, J. Zhai, Y. Song, B. Liu, L. Jiang, D. Zhu, Super-hydrophobic surfaces: from natural to artificial, Adv. Mater. 14 (2002) 1857–1860, https://doi.org/10.1002/adma.200290020.
[6] R.N. Wenzel, Resistance of solid surfaces to wetting by water, Ind. Eng. Chem. 28 (1936) 988–994, https://doi.org/10.1021/ie50320a024.
[7] A.B.D. Cassie, S. Baxter, Wettability of porous surfaces, Trans. Faraday Soc. 40 (1944) 546–551, https://doi.org/10.1039/TF9444000546.
[8] J.T. Simpson, S.R. Hunter, T. Aytug, Superhydrophobic materials and coatings: a review, Reports Prog. Phys. (2015) 78, https://doi.org/10.1088/0034-4885/78/8/086501.
[9] M.A.C. Stuart, W.T.S. Huck, J. Genzer, M. Müller, C. Ober, M. Stamm, G. B. Sukhorukov, I. Szleifer, V.V. Tsukruk, M. Urban, F. Winnik, S. Zauscher, I. Luzinov, S. Minko, Emerging applications of stimuli-responsive polymer materials, Nat. Mater. 9 (2010) 101–113, https://doi.org/10.1038/nmat2614.
[10] D. Hegemann, H. Brunner, C. Oehr, Plasma treatment of polymers for surface and adhesion improvement, Nucl. Instruments Methods Phys. Res. Sect. B Beam Interact. with Mater. Atoms 208 (2003) 281–286, https://doi.org/10.1016/S0168-583X(03)00644-X.
[11] K. Tsougeni, N. Vourdas, A. Tserepi, E. Gogolides, C. Cardinaud, Mechanisms of oxygen plasma nanotexturing of organic polymer surfaces: from stable super hydrophilic to super hydrophobic surfaces, Langmuir 25 (2009) 11748–11759, https://doi.org/10.1021/la901072z.
[12] L. Brown, T. Koerner, J.H. Horton, R.D. Oleschuk, Fabrication and characterization of poly(methylmethacrylate) microfluidic devices bonded using surface modifications and solvents, Lab Chip 6 (2006) 66–73, https://doi.org/10.1039/b512179e.
[13] R. Dorai, M.J. Kushner, A model for plasma modification of polypropylene using atmospheric pressure discharges, J. Phys. D. Appl. Phys. 36 (2003) 666–685, https://doi.org/10.1088/0022-3727/36/6/309.
[14] J. Lai, B. Sunderland, J. Xue, S. Yan, W. Zhao, M. Folkard, B.D. Michael, Y. Wang, Study on hydrophilicity of polymer surfaces improved by plasma treatment, Appl. Surf. Sci. 252 (2006) 3375–3379, https://doi.org/10.1016/j.apsusc.2005.05.038.
[15] P. Sharma, F. Ponte, M.J. Lima, N.M. Figueiredo, J. Ferreira, S. Carvalho, Plasma etching of polycarbonate surfaces for improved adhesion of Cr coatings, Appl. Surf. Sci. (2023) 637, https://doi.org/10.1016/j.apsusc.2023.157903.
[16] W.-C. Ma, J.-R. Chiou, C. Huang, Methane/nitrogen mixture plasma assisted surface modification of polymeric materials, High Energy Chem. 57 (2023) 373–378, https://doi.org/10.1134/S001814392304015X.
[17] J. Abenojar, R. Torregrosa-Coque, M.A. Martínez, J.M. Martín-Martínez, Surface modifications of polycarbonate (PC) and acrylonitrile butadiene styrene (ABS) copolymer by treatment with atmospheric plasma, Surf. Coatings Technol. 203 (2009) 2173–2180, https://doi.org/10.1016/j.surfcoat.2009.01.037.
[18] A. Riveiro, P. Pou, J. del Val, R. Comesaña, F. Arias-González, F. Lusquiños, M. Boutinguiza, F. Quintero, A. Badaoui, J. Pou, Laser texturing to control the wettability of materials, Procedia CIRP 94 (2020) 879–884, https://doi.org/10.1016/j.procir.2020.09.065.
[19] A. Riveiro, A.L.B. Maçon, J. del Val, R. Comesaña, J. Pou, Laser surface texturing of polymers for biomedical applications, Front. Phys. 6 (2018), https://doi.org/10.3389/fphy.2018.00016.
[20] C.-M. Chan, T.-M. Ko, H. Hiraoka, Polymer surface modification by plasmas and photons, Surf. Sci. Rep. 24 (1996) 1–54, https://doi.org/10.1016/0167-5729(96)80003-3.
[21] J.P. Youngblood, T.J. McCarthy, Ultrahydrophobic polymer surfaces prepared by simultaneous ablation of polypropylene and sputtering of poly (tetrafluoroethylene) using radio frequency plasma, Macromolecules 32 (1999) 6800–6806, https://doi.org/10.1021/ma9903456.
[22] S. Guruvenket, G.M. Rao, M. Komath, A.M. Raichur, Plasma surface modification of polystyrene and polyethylene, Appl. Surf. Sci. 236 (2004) 278–284, https://doi.org/10.1016/j.apsusc.2004.04.033.
[23] T. Sun, G. Wang, L. Feng, B. Liu, Y. Ma, L. Jiang, D. Zhu, Reversible switching between superhydrophilicity and superhydrophobicity, Angew. Chemie Int. Ed. 43 (2004) 357–360, https://doi.org/10.1002/anie.200352565.
[24] M.A. Nilsson, R.J. Daniello, J.P. Rothstein, A novel and inexpensive technique for creating superhydrophobic surfaces using Teflon and sandpaper, J. Phys. D. Appl. Phys. 43 (2010) 45301, https://doi.org/10.1088/0022-3727/43/4/045301.
[25] D. Song, R.J. Daniello, J.P. Rothstein, Drag reduction using superhydrophobic sanded Teflon surfaces, Exp. Fluids 55 (2014) 1783, https://doi.org/10.1007/s00348-014-1783-8.
[26] N. Menga, R. Di Mundo, G. Carbone, Soft blasting of fluorinated polymers: the easy way to superhydrophobicity, Mater. Des. 121 (2017) 414–420, https://doi.org/10.1016/j.matdes.2017.02.074.
[27] M. Chen, H. Che, S. Yue, Exploring surface preparation for cold spraying on polymers, Surf. Coatings Technol. 450 (2022) 128993, https://doi.org/10.1016/j.surfcoat.2022.128993.
[28] J.R. Dondani, J. Iyer, S.D. Tran, Surface treatments of PEEK for osseointegration to bone, Biomolecules 13 (2023), https://doi.org/10.3390/biom13030464.
[29] B. Pidhatika, V.T. Widyaya, P.C. Nalam, Y.A. Swasono, R. Ardhani, Surface Modifications of High-Performance Polymer Polyetheretherketone (PEEK) to improve its biological performance in dentistry, Polymers 14 (2022), https://doi.org/10.3390/polym14245526.
[30] R.F.V. Rocha, L.C. Anami, T.M.B. Campos, R.M. de Melo, R.O. de A. e Souza, M. A. Bottino, Bonding of the Polymer Polyetheretherketone (PEEK) to human dentin: effect of surface treatments, Braz. Dent. J. 27 (2016) 693–699, https://doi.org/10.1590/0103-6440201600796.
[31] W. Xu, J.S. Yang, T.J. Lu, Ductility of thin copper films on rough polymer substrates, Mater. Des. 32 (2011) 154–161, https://doi.org/10.1016/j.matdes.2010.06.018.
[32] M.S. Zafar, N. Ahmed, Nanoindentation and surface roughness profilometry of poly methyl methacrylate denture base materials, Technol. Heal. Care 22 (2014) 573–581, https://doi.org/10.3233/THC-140832.
[33] M. Lampin, R. Warocquier-Clérout, C. Legris, M. Degrange, M.F. Sigot-Luizard, Correlation between substratum roughness and wettability, cell adhesion, and cell migration, J. Biomed. Mater. Res. 36 (1997) 99–108, https://doi.org/10.1002/(SICI)1097-4636(199707)36, 1<99::AID−JBM12>3.0.CO;2-E.
[34] F. Bañon, S. Martin, J.M. Vazquez-Martinez, J. Salguero, F.J. Trujillo, Predictive models based on RSM and ANN for roughness and wettability achieved by laser texturing of S275 carbon steel alloy, Opt. Laser Technol. 168 (2024) 109963, https://doi.org/10.1016/j.optlastec.2023.109963.
[35] S. S, A.K. Zuhair, M.A.M. Ali, K. Kadirgama, U.K. Dubey, S. Pujari, L.D. Sivakumar, Artificial neural network predictive modelling of laser micro-grooving for commercial pure titanium (CP Ti) Grade 2, J. Mech. Eng. (2021), https://doi.org/10.24191/Jmeche.V18i2.15157 (JMechE); Vol 18 No 2 J. Mech. Eng, https://myjms.mohe.gov.my/index.php/jmeche/article/view/15157.
[36] E. Maleki, O. Unal, Shot peening process effects on metallurgical and mechanical properties of 316 L steel via: experimental and neural network modeling, Met. Mater. Int. 27 (2021) 262–276, https://doi.org/10.1007/s12540-019-00448-3.
[37] J. Wu, Z. Huang, H. Qiao, B. Wei, Y. Zhao, J. Li, J. Zhao, Prediction about residual stress and microhardness of material subjected to multiple overlap laser shock processing using artificial neural network, J. Cent. South Univ. 29 (2022) 3346–3360, https://doi.org/10.1007/s11771-022-5158-7.
[38] E. Oranli, N. Gungoren, A. Heydari Astaraee, E. Maleki, S. Bagherifard, M. Guagliano, Numerical and experimental analysis of sand blasting on polymeric substrates, Forces Mech. 12 (2023) 100208, https://doi.org/10.1016/j.finmec.2023.100208.
[39] ISO 4288:1996 - Geometrical Product Specifications (GPS) — surface texture: profile method — rules and procedures for the assessment of surface texture, (1996). https://www.iso.org/standard/2096.html.
[40] A. Heydari Astaraee, S. Bagherifard, S. Monti, M. Guagliano, Evaluating the homogeneity of surface features induced by impact-based surface treatments, Materials 14 (2021), https://doi.org/10.3390/ma14133476.
[41] A. Heydari Astaraee, S. Bagherifard, E.A. Rajme López, M. Guagliano, Adapting shot peening for surface texturing using customized additive manufactured shots, Adv. Eng. Mater. 25 (2023) 2201730, https://doi.org/10.1002/adem.202201730.
[42] D. Kirk, Generation of air-blast shot velocity, (2007).
[43] H.Z. Li, J. Wang, J.M. Fan, Analysis and modelling of particle velocities in micro-abrasive air jet, Int. J. Mach. Tools Manuf. 49 (2009) 850–858, https://doi.org/10.1016/j.ijmachtools.2009.05.012.

[44] Z.Y. Liu, Y.B. Guo, C.Z. Huang, Kinematic modeling and deformation mechanics in shot peening of functional ceramics, Procedia Manuf 5 (2016) 508–520, https://doi.org/10.1016/j.promfg.2016.08.042.
[45] Ansys GRANTA EduPack software, ANSYS, Inc., Cambridge, UK, 2021. www.ansys.com/materials.
[46] A.F. Harris, A. Beevers, The effects of grit-blasting on surface properties for adhesion, Int. J. Adhes. Adhes. 19 (1999) 445–452, https://doi.org/10.1016/S0143-7496(98)00061-X.